Published in final edited form as:
Science. 2012 March 2; 335(6072): 1106–1110. doi:10.1126/science.1215802.

Biased signaling pathways in β_2-adrenergic receptor characterized by ^{19}F-NMR

Jeffrey J. Liu[1,#], **Reto Horst**[1,#], **Vsevolod Katritch**[1], **Raymond C. Stevens**[1,*], and **Kurt Wüthrich**[1,2,*]

[1]Department of Molecular Biology, The Scripps Research Institute, 10550 North Torrey Pines Road, La Jolla, CA 92037, USA

[2]Skaggs Institute of Chemical Biology, The Scripps Research Institute, 10550 North Torrey Pines Road, La Jolla, CA 92037, USA

Abstract

Extracellular ligand binding to G protein-coupled receptors (GPCRs) modulates G-protein and β-arrestin signaling by changing the conformational states of the cytoplasmic region of the receptor. Using site-specific ^{19}F-NMR labels in the β_2-adrenergic receptor (β_2AR) in complexes with various ligands, we observed that the cytoplasmic ends of helices VI and VII adopt two major conformational states. Changes in the NMR signals reveal that agonist binding primarily shifts the equilibrium towards the G protein specific active state of helix VI. In contrast, β-arrestin-biased ligands predominantly impact the conformational states of helix VII. The selective effects of different ligands on the conformational equilibria involving helices VI and VII provide insights into the long-range structural plasticity of β_2AR in partial and biased agonist signaling.

Signaling through G protein-coupled receptors (GPCRs) is a fundamental component of eukaryotic cellular communication. As a result, GPCRs comprise a large fraction of the "druggable proteome", with more than 30% of available pharmaceuticals targeting GPCRs (1). In performing their functions, GPCRs such as the β_2-adrenergic receptor (β_2AR) recognize a diverse array of ligands and transmit signals through the cellular membrane to cytoplasmic G-proteins. In parallel to G-protein signaling, activated β_2AR can be phosphorylated and binds to β-arrestin, initiating desensitization, endocytosis of β_2AR and β-arrestin-dependent signaling (2). A number of β_2AR ligands, including the FDA-approved β-blocker carvedilol (3) and the agonist isoetharine (4), have been shown to impart differing degrees of signaling in G-protein and arrestin pathways, a phenomenon called "functional selectivity" or "biased signaling" (5). Understanding the mechanism of biased signaling can provide leads for designing more specific and efficient drugs.

Crystal structures have been determined for β_2AR with bound inverse agonists, antagonists, and agonists (6–10), including active-state β_2AR complexes with a G-protein mimetic nanobody (8) and with a heterotrimeric G-protein (11). The β_2AR–G-protein structure, which has also been analyzed by EM (12), reveals the location of the G-protein binding site,

*To whom correspondence should be addressed: stevens@scripps.edu, wuthrich@scripps.edu.
#These authors contributed equally.

Supporting Online Material
www.sciencemag.org
Materials and Methods
Tables S1 to S2
Figure S1 to S4
References (46-54)

showing that the G-protein interacts with helices V and VI, and the intracellular loops ICL2 and ICL3, but makes no substantial contacts with helices VII and VIII (Fig. 1A,B). A comparison of inactive and active-state crystal structures of β_2AR, rhodopsin (13) and the A_{2A} adenosine receptor (14, 15) suggest a common pattern of structural differences between inactive and active states in GPCRs (Fig.1C), where a coupled motion of helices V and VI, and changes in helices III and VII are accompanied by distinct side chain rotamer switches on the cytoplasmic side of the protein (16, 17). Activation of β_2AR has been investigated previously via fluorescence-based biophysical experiments (18–25) and NMR (26), and conformational changes during receptor activation were observed in helix VI and the cytoplasmic surface.

In order to probe for subtle conformational changes involved in receptor–ligand binding (27), ^{19}F-NMR spectroscopy was employed. This highly sensitive method was used to provide information based on the observation of line shapes and chemical shifts of strategically located ^{19}F-labels in the cytoplasmic region of the receptor (Fig. 1A, B) (28). Similar approaches have previously been successfully applied to studies of a number of membrane proteins (29–31). Three native cysteine residues (Cys265$^{6.27}$, Cys327$^{7.54}$, Cys341) (32) of β_2AR (33) in the cytoplasmic region of the receptor are accessible for covalent labeling with 2,2,2 trifluoroethanethiol (TET) (31), and their NMR signals were unambiguously assigned through the use of site-specific mutagenesis of these residues and all other native cysteine residues that might be affected by TET (Fig. 2A) (34). To probe for structural changes, we primarily used singly-labeled receptors, which have reduced complexity of the ^{19}F-NMR spectra when compared with wild type $^{TET}\beta_2$AR (Fig. 2A). Cys265$^{6.27}$ and Cys327$^{7.54}$ are located at the cytoplasmic ends of helices VI and VII, respectively, both of which are known to undergo large conformational changes during receptor activation (Fig. 1C). In contrast, Cys341 is located in the non-transmembrane helix VIII at the C-terminus and β_2AR(C265A, C327S, ^{TET}C341) was observed to be unresponsive to binding of different ligands (Fig. 2B). This C-terminal probe therefore served as an internal negative control relative to Cys265$^{6.27}$ and Cys327$^{7.54}$ in studies of the effects from the binding of different pharmacological ligands.

The ^{19}F-NMR spectra ofβ_2AR(^{TET}C265, C327S, C341A) and β_2AR(C265A, ^{TET}C327, C341A) (Fig. 2C–E) show prominent changes upon addition of saturating concentrations of a collection of ligands (Table S1) which represent a full spectrum of ligand efficacy (35). In general, the signals at 280K of both β_2AR(^{TET}C265, C327S, C341A) and β_2AR(C265A, ^{TET}C341A, C327) consist of two components, suggesting that the β_2AR structure contains two independent equilibria between locally different conformations manifested at these two amino acid positions. While ligand-free and inverse agonist-bound $^{TET}\beta_2$ARs have almost identical spectra, in which the populations of C327^{I} and C265^{I} are much more prominent than those of C327^{A} and C265^{A}, spectra of $^{TET}\beta_2$AR bound to the full agonist isoproterenol exhibit approximately equal populations at both residues (Fig. 3A). Shifts of this equilibrium are observed with different agonists bound to $^{TET}\beta_2$AR, suggesting that the peaks A and I are likely to represent the active and inactive state of both helices VI and VII of β_2AR, respectively. The temperature dependence of the ^{19}F-signals with regard to line width and peak intensity (Figs. 2C–E, S4) suggests that the active state of both helices VI and VII of β_2AR exhibits a larger degree of conformational plasticity than the inactive state, i.e., the active state samples a wider range of conformers with slightly different chemical shifts, either in a static ensemble or in a manifold of conformers that also includes conformational exchange.

The ^{19}F-NMR data were analyzed with a double-Lorentzian function to obtain quantitative information on the conformational equilibria (Fig. 3A). This revealed that positions and widths of the NMR peaks remain practically unchanged for all ligands studied, and

confirmed that the major effects of agonist binding are population shifts from inactive state peaks (I) to those of active state (A). A plot of relative peak volumes for $Cys265^{A}$ versus those for $Cys327^{A}$, which represent the populations of the active state in helix VI and helix VII, respectively, reveals varying degrees of agonist-mediated shifts towards the active state manifested by $Cys265^{6.27}$ and $Cys327^{7.54}$ (Fig. 3B). For most agonists the shifts along the two axes follow the same overall trend as their reported pharmacological efficacy on G-protein activation (36). For instance, the partial agonists tulobuterol, clenbuterol and norepinephrine have a less pronounced effect on $Cys265^{6.27}$ than the full agonist isoproterenol, while the full agonist formoterol elicits a greater shift in conformational equilibrium on $Cys265^{6.27}$. These results suggest that the degree to which agonists shift the equilibrium towards the active state of helix VI results in differing G-protein signaling capacity. The antagonist/weak partial agonist alprenolol can induce a small shift on $Cys265^{6.27}$, but has a minimal effect on $Cys327^{7.54}$, in agreement with previous findings that it is a weak partial agonist (25, 37). The inverse agonist carazolol, on the other hand, induces no apparent shifts as compared to the apo form. In contrast, the two β-arrestin biased ligands, isoetharine and carvedilol, cause large shifts of the equilibria in $Cys327^{7.54}$ towards the active state. Interestingly, carvedilol, like other antagonists and inverse agonists, has little influence on the equilibrium of $Cys265^{6.27}$, while isoetharine, like other agonists, also produces a prominent shift of $Cys265^{6.27}$ towards the active state.

The large activation changes in $Cys327^{7.54}$ caused by carvedilol and isoetharine suggest that helix VII primarily impacts β-arrestin signaling pathways. This is consistent with the result of a previous study that β_2AR-phosphorylation by GPCR kinases, which is a prerequisite for β-arrestin binding, primarily targets a region directly adjacent to helix VII on helix VIII (38). Furthermore, recent crystallographic (11) and EM studies (12) of aβ_2AR–$G_{\alpha\beta\gamma}$ heterotrimer complex show that the G_α subunit makes major contact with helices V and VI of β_2AR, resulting in a 14 Å outward movement of the cytoplasmic ends of these helices, whereas there is no contact between $G_{\alpha\beta\gamma}$ and helix VII (Fig. 1A,B), suggesting that the conformational changes in helix VII are not directly involved in G-protein binding and signaling.

To further characterize the environment of $Cys327^{7.54}$ in the active state, we evaluated the effect of the water-soluble paramagnetic relaxation agent gadopentetic dimeglumine (magnevist®) (39) on individual resonances of β_2AR(C265A, ^{TET}C327, C341A) bound to isoproterenol. A comparison of the line widths of peaks A and I in the 1D ^{19}F-NMR spectra at various magnevist concentrations revealed that peak I is more susceptible to the line broadening by magnevist than peak A (Fig. S1A), indicating that $Cys327^{7.54}$ in the inactive state is more readily solvent-accessible than in the active state. This interpretation is consistent with crystal structure data, where $Cys327^{7.54}$ was found to be solvent-exposed in the carazolol-bound structure (6), but buried in the trans-membrane helix bundle of the receptor in its complexes with a nanobody (8) or the G-protein (11) (Fig. S1B).

Additional insight from analysis of the ^{19}F-NMR results can be obtained by examining the chemical structures of the agonists and their interactions with the individual helices in the β_2AR binding pocket (Fig. 4). The majority of known high-affinity adrenergic ligands have a common structural motif consisting of an aromatic “head group” and an ethanolamine “tail group”. The head group (e.g., catechol) of agonists is directly connected to the ethanolamine tail, while antagonists and inverse agonists, both of which act as competitive inhibitors to agonists and either have no impact or a negative impact on the receptor basal activity, have an additional two-atom linker between the head and tail groups. Crystal structures of the β_2AR complexes with various ligands (6–11), as well as biochemical (40–42) and modeling studies (43, 44) have established that the aromatic head groups interact with helices V and VI, while the ethanolamine tails are anchored by ionic and polar interactions at helices III

and VII (Fig. 4A and Fig. S2). For agonists, polar interactions of their head groups with helix V side chains thereby mediate an inward shift of Pro211$^{5.50}$, and subsequent conformational changes involving Ile121$^{3.40}$ and Phe282$^{6.44}$ (8) result in the activation move of the cytoplasmic tip of helix VI.

The changes observed by ^{19}F-NMR (Fig. 3) provide additional insight into correlations between the chemical structure of the ligands and their interactions with β_2AR. Binding of full agonists (such as isoproterenol and formoterol) imparts a large shift in the conformational equilibrium of both helices VI (Cys265$^{6.27}$) and VII (Cys327$^{7.54}$). Binding of partial agonists, which either completely lack (as in tulobuterol) or have much weaker (as in clenbuterol) polar features on their aromatic heads, has a smaller influence on the conformational equilibrium of helix VI than full agonists, but has almost as much impact on helix VII. In addition, the β-arrestin-biased ligands carvedilol and isoetharine, which differ from their corresponding "unbiased" prototypes (inverse agonist carazolol and full agonist isoproterenol, respectively) only in the tail moieties, strongly impact the helix VII equilibrium. A key observation is that the 1D ^{19}F-NMR spectrum of β_2AR(C265A, C327S, ^{TET}C341) bound to isoetharine, which is one of the most potent biased agonists, is similar to those of β_2AR(C265A, C327S, ^{TET}C341) bound to carazolol and isoproterenol (Fig. 2B). This shows that the C-terminus of the non-transmembrane helix VIII, where Cys341 is located, is not directly involved in the β-arrestin signaling pathway. In the absence of structural data on a complex of β_2AR with β-arrestin, it is tempting to further hypothesize from this data that the position of Cys341 on helix VIII is located outside of the interface with bound arrestin.

These observations on structure–activity relationships for β-arrestin biased β_2AR ligands, and unbiased full and partial agonists, provide insights into β_2AR signaling pathways that suggest the existence of parallel pathways for G-protein and β-arrestin signaling (Fig. S3). Although these pathways appear interconnected on several levels and may involve other activation-related rearrangements in the cytoplasmic and periplasmic loops (45), the present ^{19}F-NMR results point to a significant level of decoupling of the two pathways. The implicated links between ligand structure and function may serve as a platform for future rational design of specific ligands.

Given the above observations on the correlation between ligand structure and receptor response, a connection can now be made between the chemical structures of pharmacological ligands and their signaling pathways acting either through G-proteins or β-arrestins. The general principle that links the chemical space of the ligands to the specific changes in conformational plasticity at the signaling cytoplasmic receptor surface may be preserved in other GPCRs. The use of ^{19}F-NMR may thus prove to be a widely applicable tool for structure–activity relationship studies of GPCR ligands.

Supplementary Material

Refer to Web version on PubMed Central for supplementary material.

Acknowledgments

This work was supported in part by NIH Roadmap Initiative grant P50 GM073197 for technology development and purchase of the ^{19}F-NMR probe, and by PSI:Biology grant U54 GM094618 for GPCR biology studies. The authors thank J. Velasquez for help on molecular biology; C. Cornillez-Ty, T. Trinh, and K. Allin for help on baculovirus expression; J. Gatchalian for ligand binding assays; P. Stanczak for assistance with the paramagnetic titration experiment; V. Cherezov for helpful discussions; I. Wilson for careful review and scientific feedback on the manuscript; K. Kadyshevskaya for assistance with figure preparation; and A. Walker for assistance with manuscript preparation. R.C.S. is a founder and member of the board of directors of Receptos, a GPCR structure-based drug discovery company.

References and Notes

1. Hopkins AL, Groom CR. The druggable genome. Nat Rev Drug Discov. 2002; 1:727. [PubMed: 12209152]
2. Rajagopal K, Lefkowitz RJ, Rockman HA. When 7 transmembrane receptors are not G protein-coupled receptors. J Clin Invest. 2005; 115:2971. [PubMed: 16276410]
3. Shenoy SK, Lefkowitz RJ. beta-arrestin-mediated receptor trafficking and signal transduction. Trends Pharmacol Sci. 2011; 32:521. [PubMed: 21680031]
4. Drake MT, et al. beta-arrestin-biased agonism at the beta2-adrenergic receptor. J Biol Chem. 2008; 283:5669. [PubMed: 18086673]
5. Urban JD, et al. Functional selectivity and classical concepts of quantitative pharmacology. J Pharmacol Exp Ther. 2007; 320:1. [PubMed: 16803859]
6. Cherezov V, et al. High-resolution crystal structure of an engineered human beta2-adrenergic G protein-coupled receptor. Science. 2007; 318:1258. [PubMed: 17962520]
7. Hanson MA, et al. A specific cholesterol binding site is established by the 2.8 A structure of the human beta2-adrenergic receptor. Structure. 2008; 16:897. [PubMed: 18547522]
8. Rasmussen SG, et al. Structure of a nanobody-stabilized active state of the beta(2) adrenoceptor. Nature. 2011; 469:175. [PubMed: 21228869]
9. Rosenbaum DM, et al. Structure and function of an irreversible agonist-beta(2) adrenoceptor complex. Nature. 2011; 469:236. [PubMed: 21228876]
10. Wacker D, et al. Conserved binding mode of human beta2 adrenergic receptor inverse agonists and antagonist revealed by X-ray crystallography. J Am Chem Soc. 2010; 132:11443. [PubMed: 20669948]
11. Rasmussen SG, et al. Crystal structure of the beta2 adrenergic receptor-Gs protein complex. Nature. 2011; 477:549. [PubMed: 21772288]
12. Westfield GH, et al. Structural flexibility of the G{alpha}s {alpha}-helical domain in the {beta}2-adrenoceptor Gs complex. Proc Natl Acad Sci U S A. 2011; 108:16086. [PubMed: 21914848]
13. Scheerer P, et al. Crystal structure of opsin in its G-protein-interacting conformation. Nature. 2008; 455:497. [PubMed: 18818650]
14. Jaakola VP, et al. Identification and characterization of amino acid residues essential for human A2A adenosine receptor : ZM241385 binding and subtype selectivity. J Biol Chem. 2010; 285:13032. [PubMed: 20147292]
15. Xu F, et al. Structure of an Agonist-Bound Human A2A Adenosine Receptor. Science. 2011; 332:322. [PubMed: 21393508]
16. Deupi X, Standfuss J. Structural insights into agonist-induced activation of G-protein-coupled receptors. Curr Opin Struct Biol. 2011; 21:541. [PubMed: 21723721]
17. Nygaard R, Frimurer TM, Holst B, Rosenkilde MM, Schwartz TW. Ligand binding and micro-switches in 7TM receptor structures. Trends Pharmacol Sci. 2009; 30:249. [PubMed: 19375807]
18. Gether U, et al. Structural instability of a constitutively active G protein-coupled receptor. Agonist-independent activation due to conformational flexibility. J Biol Chem. 1997; 272:2587. [PubMed: 9006889]
19. Ghanouni P, et al. Functionally different agonists induce distinct conformations in the G protein coupling domain of the beta 2 adrenergic receptor. J Biol Chem. 2001; 276:24433. [PubMed: 11320077]
20. Ghanouni P, Steenhuis JJ, Farrens DL, Kobilka BK. Agonist-induced conformational changes in the G-protein-coupling domain of the beta 2 adrenergic receptor. Proc Natl Acad Sci U S A. 2001; 98:5997. [PubMed: 11353823]
21. Granier S, et al. Structure and conformational changes in the C-terminal domain of the beta2-adrenoceptor: insights from fluorescence resonance energy transfer studies. J Biol Chem. 2007; 282:13895. [PubMed: 17347144]
22. Swaminath G, et al. Probing the beta2 adrenoceptor binding site with catechol reveals differences in binding and activation by agonists and partial agonists. J Biol Chem. 2005; 280:22165. [PubMed: 15817484]

23. Swaminath G, et al. Sequential binding of agonists to the beta2 adrenoceptor. Kinetic evidence for intermediate conformational states. J Biol Chem. 2004; 279:686. [PubMed: 14559905]
24. Yao X, et al. Coupling ligand structure to specific conformational switches in the beta2-adrenoceptor. Nat Chem Biol. 2006; 2:417. [PubMed: 16799554]
25. Yao XJ, et al. The effect of ligand efficacy on the formation and stability of a GPCR-G protein complex. Proc Natl Acad Sci U S A. 2009; 106:9501. [PubMed: 19470481]
26. Bokoch MP, et al. Ligand-specific regulation of the extracellular surface of a G-protein-coupled receptor. Nature. 2010; 463:108. [PubMed: 20054398]
27. Danielson MA, Falke JJ. Use of 19F NMR to probe protein structure and conformational changes. Annu Rev Biophys Biomol Struct. 1996; 25:163. [PubMed: 8800468]
28. See supporting material and methods on Science Online.
29. Evanics F, Kitevski JL, Bezsonova I, Forman-Kay J, Prosser RS. 19F NMR studies of solvent exposure and peptide binding to an SH3 domain. Biochim Biophys Acta. 2007; 1770:221. [PubMed: 17182189]
30. Falke JJ, Luck LA, Scherrer J. 19F nuclear magnetic resonance studies of aqueous and transmembrane receptors. Examples from the Escherichia coli chemosensory pathway. Biophys J. 1992; 62:82. [PubMed: 1318106]
31. Klein-Seetharaman J, Getmanova EV, Loewen MC, Reeves PJ, Khorana HG. NMR spectroscopy in studies of light-induced structural changes in mammalian rhodopsin: applicability of solution (19)F NMR. Proc Natl Acad Sci U S A. 1999; 96:13744. [PubMed: 10570143]
32. Ballesteros-Weistein numbering is shown as a superscript. The most conserved residue in each transmembrane helix is designated as x.50, where x is the number of the transmembrane helix, and the second number (50) indicates the relative position of the specific residue. The second number decreases towards the N terminus and vice versa. Only residues on transmembrane helices are noted.
33. In order to produce β_2AR samples that are stabilized enough for NMR measurement, the C-terminus was truncated, the part of intracellular loop 3 that is not involved in G-protein recruitment was removed, and a stabilizing E122W mutation was added. Constructs containing these modifications were also crystallized and characterized as functionally similar to the unmodified β_2AR.
34. The three ^{19}F-signals in labeled wild type $^{TET}\beta_2$AR/carazolol were identified by comparison with signals from β_2AR constructs containing single labeled residues, i.e., β_2AR(^{TET}C265, C327S, C341A), β_2AR(C265A, ^{TET}C327, C341A) and β_2AR(C265A, C327S, ^{TET}C341).
35. Ligand binding properties of the cysteine mutants were examined on the membranes from β_2AR expressing *Sf9* cells. Radioligand binding assay used [^{3}H]Dihydroalprenolol as the reporter ligand, and competition assay used isoproterenol as the competing ligand. The binding affinity of antagonist to the wild type receptor (1.4 nM) is identical to all cysteine mutants (Cys(265) = 1.1 ± 0.1 nM, Cys(327) = 1.4 ± 0.4 nM, Cys(341) = 1.1 ± 0.1 nM) and the affinity of full agonist to the wild type receptor (323 nM) is similar to all cysteine mutants (Cys(265) = 100nM, Cys(327) = 118nM, Cys(341) = 138nM).
36. Baker JG. The selectivity of beta-adrenoceptor agonists at human beta1-, beta2- and beta3-adrenoceptors. Br J Pharmacol. 2010; 160:1048. [PubMed: 20590599]
37. Wisler JW, et al. A unique mechanism of beta-blocker action: carvedilol stimulates beta-arrestin signaling. Proc Natl Acad Sci U S A. 2007; 104:16657. [PubMed: 17925438]
38. Nobles KN, et al. Distinct phosphorylation sites on the beta(2)-adrenergic receptor establish a barcode that encodes differential functions of beta-arrestin. Sci Signal. 2011; 4:ra51. [PubMed: 21868357]
39. Hilty C, Wider G, Fernandez C, Wuthrich K. Membrane protein-lipid interactions in mixed micelles studied by NMR spectroscopy with the use of paramagnetic reagents. Chembiochem. 2004; 5:467. [PubMed: 15185370]
40. Liapakis G, et al. The forgotten serine. A critical role for Ser-2035.42 in ligand binding to and activation of the beta 2-adrenergic receptor. J Biol Chem. 2000; 275:37779. [PubMed: 10964911]

41. Strader CD, Candelore MR, Hill WS, Sigal IS, Dixon RA. Identification of two serine residues involved in agonist activation of the beta-adrenergic receptor. J Biol Chem. 1989; 264:13572. [PubMed: 2547766]

42. Strader CD, et al. Conserved aspartic acid residues 79 and 113 of the beta-adrenergic receptor have different roles in receptor function. J Biol Chem. 1988; 263:10267. [PubMed: 2899076]

43. de Graaf C, Rognan D. Selective structure-based virtual screening for full and partial agonists of the beta2 adrenergic receptor. J Med Chem. 2008; 51:4978. [PubMed: 18680279]

44. Katritch V, et al. Analysis of full and partial agonists binding to beta2-adrenergic receptor suggests a role of transmembrane helix V in agonist-specific conformational changes. J Mol Recognit. 2009; 22:307. [PubMed: 19353579]

45. Kahsai AW, et al. Multiple ligand-specific conformations of the beta(2)-adrenergic receptor. Nat Chem Biol. 2011; 7:692. [PubMed: 21857662]

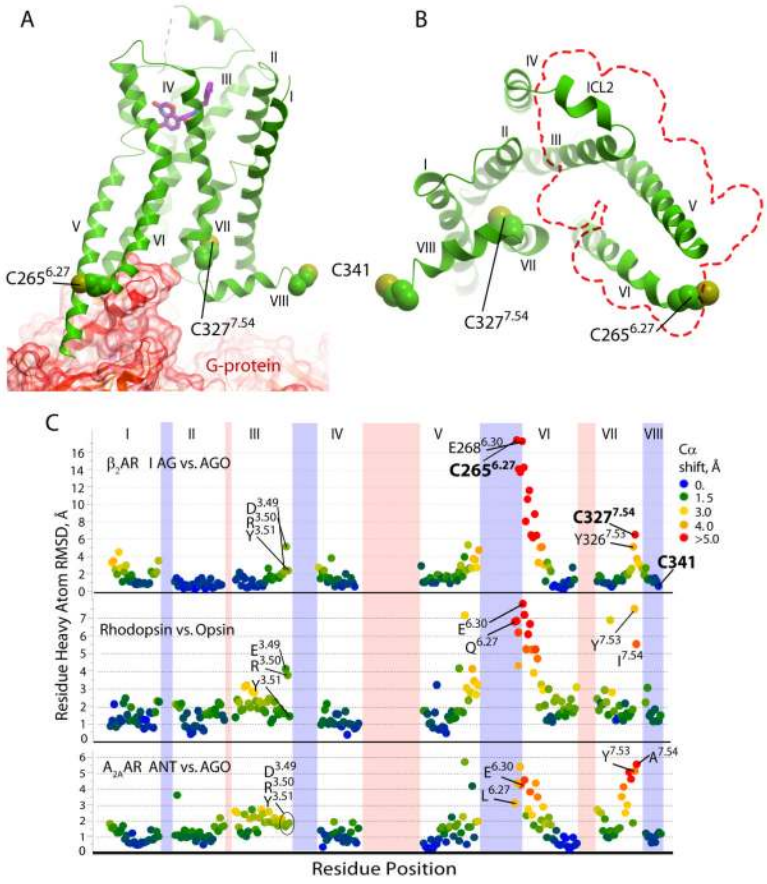

Fig. 1.

Locations of ^{19}F-NMR labels in β_2AR and activation-related changes in GPCR crystal structures. (**A**) Side view of β_2AR in the active G protein-bound form (PDB ID 3SN6, shown in green). The trans-membrane helices I to VII and the C-terminal helix VIII are identified. The full agonist BI-167107 in the ligand-binding site is shown as a stick diagram. Green and yellow spheres highlight the three cysteine residues used for TET labeling, i.e., Cys265$^{6.27}$ and Cys327$^{7.54}$ at the cytoplasmic ends of helices VI and VII, respectively and Cys341 at the C-terminus. The bound G-protein heterotrimer is shown as red ribbons and surfaces. (**B**) Cytoplasmic view of the structure in (**A**), with the G-protein contact sites outlined by a broken red line**.** (**C**) Plot of distance root mean square deviations (RMSD) of individual residues between crystal structures of inactive and active-states of three GPCRs. Crystal structures used (from top to bottom): β_2AR (PDB IDs 2RH1 vs. 3SN6), rhodopsin (PDB IDs 1GZM vs. 3DQB), A_{2A} adenosine receptor (A_{2A}AR; PDB IDs 3EML vs. 3QAK). The horizontal axes represent the amino acid sequences (β_2AR residues 34–341, bovine rhodopsin residues 38–320, A_{2A}AR residues 6–302). The vertical axis shows all-heavy-atom RMSDs per residue, while the color code defined in the upper right corner of the panel indicates corresponding C$^{\alpha}$ deviations. For each protein, selected residues are identified (see text). The locations of the helices I to VIII are indicated at the top. Periplasmic loop regions are highlighted in red, while cytoplasmic loops and helix VIII are highlighted in blue. The cytoplasmic ends of helices VI and VII, which contain Cys265$^{6.27}$ and Cys327$^{7.54}$, are “hot spots” with large conformational rearrangements between the crystal structures of inactive and active states; other transmembrane helices and intracellular helix VIII, which includes Cys341, show only small displacements.

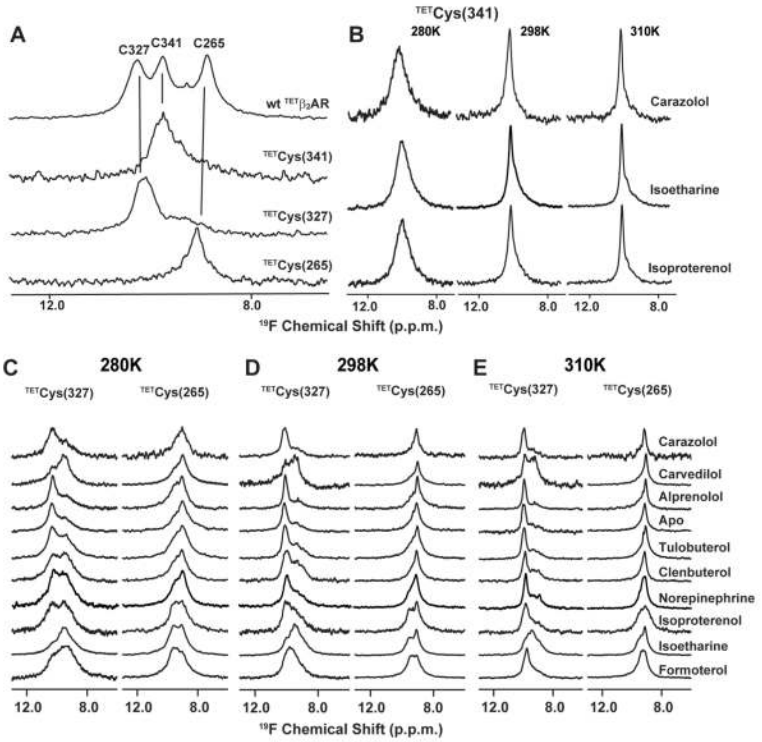

Fig. 2.

1D ^{19}F-NMR spectra of different TET-labeled β_2AR constructs under variable solution conditions. (**A**) ^{19}F-NMR resonance assignments for carazolol-bound $^{TET}\beta_2$AR at 298 K. Spectra of the following constructs were recorded: wt $^{TET}\beta_2$AR; β_2AR (^{TET}C265, C327S, C341A), β_2AR (C265A, ^{TET}C327, C341A) and β_2AR (C265A, C327S, ^{TET}C341). The vertical lines connect peaks in the ^{19}F-NMR spectrum of $^{TET}\beta_2$AR with the corresponding peaks in the spectra of the single-residue TET-labeled mutants. At the top, the peak assignments are indicated by the one-letter amino acid code and the residue number. (**B**) β_2AR (C265A, C327S, ^{TET}C341) in complex with an inverse agonist (carazolol), a biased agonist (isoetharine), and a full agonist (isoproterenol) at 280K, 298K and 310K. (**C**), (**D**) and (**E**) β_2AR (^{TET}C265, C327S, C341A) and β_2AR (C265A, ^{TET}C327, C341A) free and bound to nine different ligands at 280K, 298K and 310K. In (**B**) to (**E**), the temperature and the ligands are indicated at the top and on the right, respectively. For all experiments, the following parameter settings were used to collect and process the spectra: data size 1024 complex points, acquisition time 51 ms, 24576 scans per increment. The data were multiplied with an exponential function with a line-broadening factor of 30 Hz, and zero-filled to 2048 points prior to Fourier transformation.

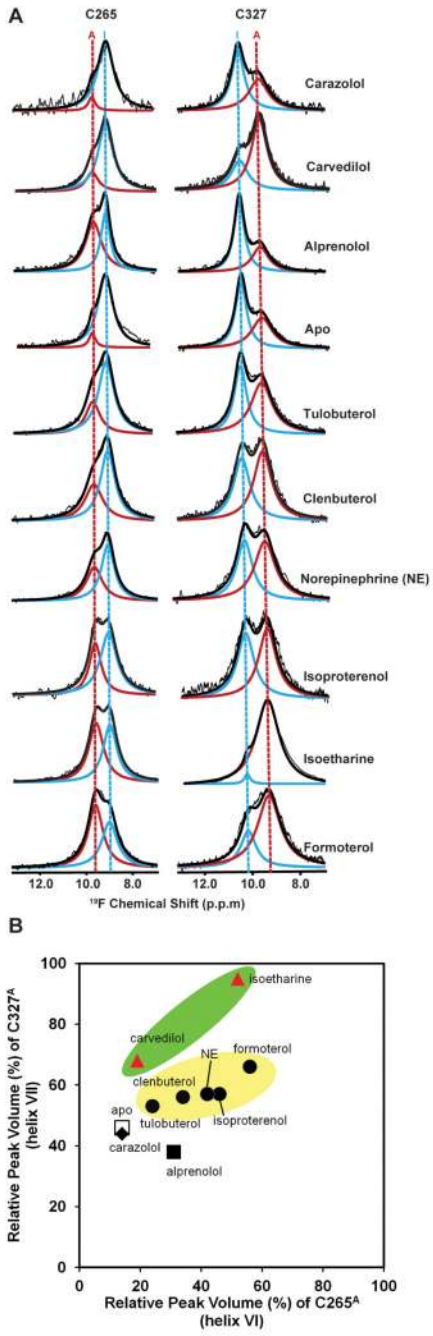

Fig. 3.

Relative populations of active (A, red) and inactive (I, blue) states of β_2AR derived from the 1D ^{19}F-NMR spectra at 280K. (**A**) Peak volumes for the individual components in the 1D ^{19}F-NMR signals of β_2AR (^{TET}C265, C327S, C341A) and β_2AR(C265A, ^{TET}C327, C341A) obtained by a non-linear least-squares fit to a double-Lorentzian function. The experimental data and the double-Lorentzian are indicated by thin and thick black lines, respectively. The fit used the chemical shift positions of peaks A and I indicated by the red and blue vertical lines. (**B**) Plot of the relative peak volumes for C265^A versus the relative peak volumes for C327^A. The relative peak volumes are the ratios of the volume of peak A and the sum of the volumes of peaks A and I. Agonists (tulobuterol, clenbuterol,

norepinephrine (NE), isoproterenol, formoterol) are shown as black circles highlighted by a yellow background, biased ligands (carvedilol, isoetharine) as red triangles highlighted by a green background, a neutral antagonist (alprenolol) as a black square, an inverse agonist (carazolol) as a black diamond, and the apo-protein as an open square.

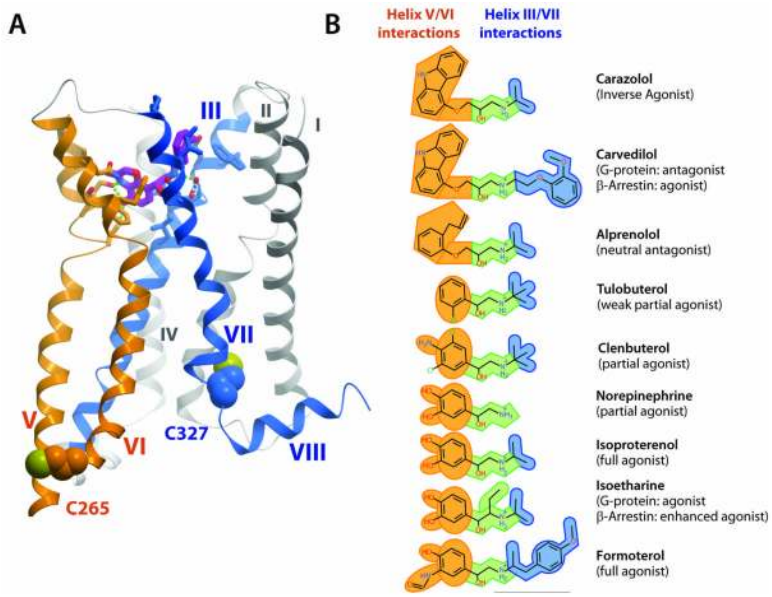

Fig. 4.

Features of ligand binding in the β_2AR structure and a conceptual model of signaling pathways to G-proteins and arrestins in β_2AR activation. **(A)** Side view of the structure of active-state β_2AR in the complex with the agonist BI-167107 (PDB ID 3SN6), with helices V/VI and III/VII color-coded orange and blue, respectively, to indicate that they interact with the correspondingly colored fragments of the ligands in **(B)**. (**B**) Chemical structures of the ligands used in the current ^{19}F-NMR studies. Orange highlights the head groups, green the common ethanolamine moieties and blue the substituents to the amino group of the ethanolamine tail. Ligand names are shown on the right, with published pharmacological efficacy indicated in parentheses.